Numerical Simulation of Unsteady Flows Generated by Dissociating Nitrogen Diffusion

Lionel Marraffa*
Office National d'Etudes et de Recherches Aéronautiques, Chatillon, France
George S. Dulikravich†
Pennsylvania State University, University Park, Pennsylvania
and
George S. Deiwert‡
NASA Ames Research Center, Moffett Field, California

An explicit time accurate predictor-corrector scheme, similar to MacCormack's, has been used to simulate unsteady nonequilibrium laminar chemically-reacting diffusion-reaction generated flows. A zonal approach, along with nonstructured boundaries, allows computation of internal and external flow with the same computer code. Results for equilibrium flows generated by dissociating, vibrationally relaxing nitrogen in a rectangular chamber are presented. The unsteady flows were generated strictly by the chemical reactions and concentration gradients.

Nomenclature

C = atomic concentration of N
C_p = specific heat at constant pressure
D = computational domain or subdomain (also diffusion coefficient)
E_{vib} = vibrational energy of diatomic molecules
e = internal energy per unit mass
h = enthalpy per unit mass
h_t = total enthalpy per unit mass
$\mathbf{I}$ = identity tensor
k = reaction rate constant (also, Boltzmann constant)
K = equilibrium constant
L_e = Lewis number: $L_e = \rho C_p D/\lambda$
m = specie molar mass
$\tilde{m}$ = mixture molar mass: $\tilde{m} = (\sum_{s=1}^{n_s} m_s X_s)/(\sum_{s=1}^{n_s} X_s)$
$\boldsymbol{n}$ = unit vector normal to a surface pointing to the exterior
n_s = number of species
P = thermodynamic pressure
P_r = Prandtl number $P_r = \mu C_p/\lambda$
$\underline{q}$ = total heat flux
R = gas constant
T = absolute temperature
$\underline{u}$ = velocity vector
$\underline{u}'$ = grid displacement velocity
v = specific volume
X = chemical (molar) concentration
$\dot{X}_{react}$ = species source term due to chemical reactions

Greek Letters

$\Delta H'_{fi}$ = (or ΔH_{fi}) enthalpy of formation of diatomic (monoatomic) specie
θ_v = characteristic temperature for vibration of a diatomic specie
λ = thermal conductivity
μ = coefficient of shear viscosity
μ_B = coefficient of bulk viscosity
ρ = density
τ = viscous stress tensor
τ_v = vibrational relaxation time

Symbols

d/dt = Lagrangian derivative
$\partial/\partial t$ = Eulerian derivative
$\delta/\delta t = \delta_t$ = time derivative following a point
$\times$ = vector or tensor product
Π = product

Subscripts

b = backward reaction
(eq) = equilibrium
f = formation (also forward reaction)
s = monatomic or diatomic specie
t = total

Superscript

0 = initial
t = transpose of a matrix

Introduction

ACCURATE prediction of all aspects of hypersonic flows around realistic configurations recently has been emphasized in several projects.[1-3]

At the very high Mach numbers, behind a strong shock, air is dissociating, vibrationally excited, and out of equilibrium. Moreover, radiative effects can become very important,[4] and ionization can develop. Very few experimental data are available, and very few facilities are able to reach the operating range of these new vehicles. Thus, one has to use sophisticated computer codes to predict the complex aerothermal fields around such hypersonic vehicles from the limited amount of data available. Perfect (nonreacting) equilibrium flow computations are available[5-7] and have been successfully compared with experimental data for simple geometries.[8] Nonequilibrium reactive flow computations,[9] with radiative effects,[10] have been recently made possible because of the availability of new supercomputers. These computations are very time consuming, and some attempts have been made to apply parabolized Navier Stokes codes,[11,12] to nonequilibrium flows.

Presented as Paper 87-2549 at the AIAA 5th Applied Aerodynamics Conference, Monterey, CA, Aug. 17-19, 1987; received Nov. 23, 1987; revision received June 3, 1988.

*Research Scientist, Aerodynamics Department.
†Associate Professor, Department of Aerospace Engineering.
‡Chief, Aerothermodynamics Branch.

Park[13] has shown the need for a two-temperature model for the correct representation of chemical rates. Most of the available codes do not take into account vibrational relaxation, thus limiting either their range of applications or their accuracy.

The code that we present in this paper gives the time dependent solution for a two-dimensional flow of multicompositional reacting gas. It takes into account vibrational relaxation of diatomic molecules and nonequilibrium chemistry. The code is capable of treating internal or external diffusion-generated laminar flows. Provision has been made for possible displacements of the grid points, allowing the use of optimal grids.[14] An explicit MacCormack scheme[15] has been chosen for its suitability for vector computation and its high time accuracy. The use of nonstructured boundaries, as well as a zonal approach, allows for more versatile applications.

Governing Equations

When the body forces, electromagnetic and radiative effects, are neglected, then the species continuity, momentum, and energy equations can be written in a compact form as

$$\frac{\delta X_i}{\delta t} + \nabla \cdot (X_i \underline{u}) - \underline{u}' \cdot \nabla X_i = \nabla \cdot \left(\rho D_i \nabla \frac{X_i}{\rho} \right) + \dot{X}_{i_{\text{react}}} \qquad i = 1,\ldots,n_s \tag{1}$$

$$\frac{\delta \rho \underline{u}}{\delta t} + \nabla \cdot (\rho \underline{u} \times \underline{u} + P\mathbf{I} - \tau) - \underline{u}' \cdot \nabla \rho \underline{u} = 0 \tag{2}$$

$$\frac{\delta \rho e_t}{\delta t} + \nabla \cdot (\rho \underline{u} e_t + \underline{q} + P\underline{u} - \tau \cdot \underline{u}) - \underline{u}' \cdot \nabla \rho e_t = \sum_i \nabla \cdot \left[(\rho h_i) \left(\frac{\rho D_i}{X_i} \nabla \frac{X_i}{\rho} \right) \right] + \Delta H_{\text{react}} \tag{3}$$

This system must be complemented by the vibrational energy equations, for each diatomic specie

$$\frac{\delta E^i_{\text{vib}}}{\delta t} + \nabla \cdot (E^i_{\text{vib}} \underline{u}') - \underline{u}' \cdot \nabla E^i_{\text{vib}} = \frac{E^{i\,(eq)}_{\text{vib}} - E^i_{\text{vib}}}{\tau_{ii}} \tag{4}$$

$$\rho h_t = \sum_{i=1}^{n_s} \rho h_i \tag{11}$$

These governing equations include the term $\underline{u}' \cdot \nabla \{\underline{X}_i, \rho \underline{u}, \rho e_t, \underline{E}^i_{\text{vib}}\}^t$.

This term is similar to the one introduced by Brackbill,[16] and allows movements of the computational grid as a function of time. Optimized solution adaptive composite grids could be used, such as the one developed by Kennon et al.[14]

Thermodynamic and Transport Properties

The specific heat of the mixture is obtained from

$$C_p = \sum m_i X_i C_{pi} \tag{12}$$

where C_{pi} is the specific heat at constant pressure of component i at the temperature T of the mixture. C_{pi} is obtained by interpolation of thermodynamics data from Miner and Lewis.[17] For each species, the viscosity μ_i is given by a curve fit relation

$$\mu_i = 10^{-1} \exp(C_i) T^{(A_i \ell n T + B_i)} (\text{kg m}^{-1}\,\text{s}^{-1}) \tag{13}$$

Here, T is the absolute temperature in K, μ_i is the viscosity; and A_i, B_i, and C_i are given by Miner and Lewis.[17] Then, μ_ℓ for laminar flow is obtained by Wilke's semiempirical[18] relations

$$\mu_\ell = \sum_{i=1}^{n_s} \frac{x_i \mu_i}{\sum_{j=1}^{n_s} x_i \Phi_{ij}} \tag{14}$$

where

$$x_i = X_i \bar{m}/m_i \tag{15}$$

$$\Phi_{ij} = \left[1 + \left(\frac{\mu_i}{\mu_j} \right)^{1/2} \left(\frac{m_j}{m_i} \right)^{1/4} \right]^2 \left[\sqrt{8} \left(1 + \frac{m_i}{m_j} \right)^{1/2} \right]^{-1} \tag{16}$$

Similarly, we obtain[18] the coefficient of heat conductivity λ for each specie i from

$$\lambda_i = \frac{\mu_i k}{m_i} \left(\frac{C_{pi} m_i}{R} + \frac{5}{4} \right) \tag{17}$$

The variables that we use are: $\underline{X}_i$, $\rho\underline{u}$, ρe_t, and $\underline{E}^i_{\text{vib}}$. This system also needs the following state relations and definitions:

$$P = \left(\sum_{s=1}^{n_s} X_s\right) RT \tag{5}$$

$$\rho = \sum_{s=1}^{n_s} m_s X_s \tag{6}$$

$$\tau = \mu(\nabla \underline{u} + \nabla \underline{u}^t) + \left(\mu_B - \frac{2}{3}\mu\right)(\nabla \cdot \underline{u})\mathbf{I} \tag{7}$$

For monatomic species

$$\rho h_i = X_i\left(\frac{5}{2} RT\right) + m_i X_i \frac{u^2}{2} \tag{8}$$

For diatomic species

$$\rho h_i = X_i\left(\frac{7}{2} RT + E^i_{\text{vib}}\right) + m_i X_i \frac{u^2}{2} \tag{9}$$

$$\Delta H_{\text{react}} = \sum_{i=1}^{n_s} \dot{X}_{i_{\text{react}}} \Delta H_{fi} \tag{10}$$

Then, the total thermal conductivity for laminar flows is

$$\lambda = \sum_{i=1}^{n_s} \frac{x_i \lambda_i}{\sum_{j=1}^{n_s} x_i \Phi_{ij}} \tag{18}$$

The diffusion coefficient is obtained from

$$D_i = \frac{\lambda Le_i}{\rho C_p} \tag{19}$$

where Le_i is the Lewis number of specie i, assumed to be constant[17] and equal to 1.4.

Chemistry

Near a strong shock wave, the vibrational temperature is not at its equilibrium value and can be very different from the translational temperature. Park[13] has shown the importance of the correct evaluation of this temperature for the purpose of computing the chemical rate coefficients. An approximation of the model of vibrational relaxation of Landau and Teller, detailed by Vincenti and Kruger,[19] has been adopted. In this model the relaxation time τ_v is given by

$$\tau_v = A \frac{\exp(k_2/T)^{1/3}}{P} \tag{20}$$

and the equilibrium vibrational energy is

$$E_{\text{vib}}^{(eq)} = \frac{\theta_v R}{\exp(\theta_v/T) - 1} \tag{21}$$

The values of constants A, k_2, and θ_v can be found in Vincenti and Kruger.[19]

Even though the governing equations take into account any number of monatomic or diatomic species, the results shown correspond to a system of two chemical species: N_2 and N. The relevant reactions are dissociations of N_2 with N or N_2 as catalysers.

$$N_2 + N \underset{k_{1b}}{\overset{k_{1f}}{\rightleftarrows}} 2N + N \tag{22}$$

$$N_2 + N_2 \underset{k_{2b}}{\overset{k_{2f}}{\rightleftarrows}} 2N + N_2 \tag{23}$$

Equations governing the evolution of the concentration X_1 of N, and X_2 of N_2, starting from a given initial state (X_1^o, X_2^o), are obtained by introducing the equilibrium constant K from Eqs. (22) and (23).

$$\frac{dX_1}{dt} = 2(k_{1b}X_1 + k_{2b}X_2)(KX_2 - X_1^2) \tag{24}$$

$$X_1^o + 2X_2^o = C = X_1 + 2X_2 \tag{25}$$

If a time step Δt is used for governing equations (1–4), the integration of Eqs. (24) and (25) will give the concentrations $X_1(\Delta t)$ and $X_2(\Delta t)$ after Δt. Therefore, the source terms are

$$\dot{X}_{i_{\text{react}}}\Delta t = X_i(\Delta t) - X_i^o, \qquad i = 1,2 \tag{26}$$

The reaction rate constants k_{1b}, k_{2b} and the equilibrium constant K, based on concentration, are dependent on temperature T and are obtained from Rakich et al.[20]

$$k_i(T) = a_i T^{si} \exp\left(-\frac{Td_i'}{T}\right), \qquad i = 1,2 \tag{27}$$

$$K = (A_1 + A_2 T + A_3 T^2) \exp\left(-\frac{Td}{T}\right) \tag{28}$$

Since MacCormack's explicit scheme is used, source terms are evaluated at time step n, where the temperature T is known everywhere.

In the most general case, with a large number of species, the system of ordinary differential equations obtained for the evaluation of the concentration needs to be solved numerically. Moreover, its stiffness makes it necessary to use appropriate routines such as DGEAR[21] from the standard IMSL library of mathematical subroutines or the one proposed by Radhakrishnan.[22]

But in the case of two species, the system can be integrated exactly as detailed next. Substituting Eq. (25) into Eq. (24), one obtains

$$\frac{dX_1}{dt} = -2\left[\left(k_{1b} - \frac{k_{2b}}{2}\right)X_1 + k_{2b}\frac{C}{2}\right]\left(X_1^2 + K\frac{X_1}{2} - \frac{KC}{2}\right) \tag{29}$$

Let us introduce

$$\Delta = \frac{K^2}{4} + 2KC, \qquad b = \frac{K/2 + \sqrt{\Delta}}{2},$$

$$d = \frac{K/2 - \sqrt{\Delta}}{2} = -X_1^{eq} \tag{30}$$

Then if $2k_{1b} \neq k_{2b}$ the solution X_1 obeys

$$f(X_1) = f(X_1^0)e^{-k_{2b}/a(t - t_o)} \tag{31}$$

where $a = k_{2b}/(2k_{1b} - k_{2b})$ and

$$f(X_1^0) = |X_1 + a|^{(a-b)(a-d)} \cdot |X_1 + b|^{(b-a)(b-d)} \cdot |X_1 + d|^{(d-a)(d-b)} \tag{32}$$

If $2k_{1b} = k_{2b}$, the solution X_1 must obey

$$g(X_1) = g(X_1^0)e^{-k_{2b}C(t - t_0)} \tag{33}$$

where

$$g(X_1^0) = |(X_1 + b)(X_1 + d)|^{(d-b)} \tag{34}$$

In both cases, X_1 is given by an implicit relation. These relations are easily solved in a few Newton iterations, with a high precision. Moreover, an adequate change of variable can significantly improve the convergence rate of the iterative method. For example, introducing

$$\alpha = \frac{X_1^0 - X_1^{eq}}{X_1 - X_1^{eq}} \tag{35}$$

where the superscript eq refers to the equilibrium value of X_1, we can define $\phi(\alpha) = \log[f(X)]$. Then

$$X_1 = X_1^{eq} + \frac{X_1^0 - X_1^{eq}}{\alpha} \tag{36}$$

$$\phi(\alpha) = (a-b)(a-d)\log\left|(X_1^{eq} + a) + \frac{X_1^0 - X_1^{eq}}{\alpha}\right| + (b-a)(b-d)\log\left|(X_1^{eq} + b) + \frac{X_1^0 - X_1^{eq}}{\alpha}\right| + (d-a)(d-b)\log\left|(X_1^{eq} + d) + \frac{X_1^0 - X_1^{eq}}{\alpha}\right| \tag{37}$$

We want to find α such that [from Eq. (31)]

$$\phi(\alpha) = -(k_{2b}/a)(t - t_0) \tag{38}$$

Notice that $\phi(\alpha)$ also can be considered as a function $\psi(u)$, of $u = \log \alpha$. Thus, we have to find $\alpha = e^u$, verifying that

$$\phi(\alpha) = \psi(u) = -k_{2b}/a(t - t_o) \tag{39}$$

We can apply Newton's method to find u (or α)

$$\kappa(\alpha) = \frac{\partial\psi}{\partial u} = \frac{(a-b)(a-d)}{1 + \alpha\left(\dfrac{X_1^{eq} + a}{X_1^0 - X_1^{eq}}\right)} + \frac{(b-a)(b-d)}{1 + \alpha\left(\dfrac{X_1^{eq} + b}{X_1^0 - X_1^{eq}}\right)} + (d-a)(d-b) \tag{40}$$

The objective is to solve

$$\phi(\alpha) = \psi(u) = -(k_{2b}/a)(t - t_0) = h \tag{41}$$

Newton's method, applied to u, yields an iteration of the type

$$u^{n+1} = u^n + \frac{h - \psi(u)}{\partial\psi/\partial u} \tag{42}$$

Thus

$$\alpha^{n+1} = \alpha^n \exp\left(\frac{h - \phi(\alpha)}{\kappa(\alpha)}\right) \tag{43}$$

Such an iteration converges considerably faster than the primitive Newton's method applied to X_1.

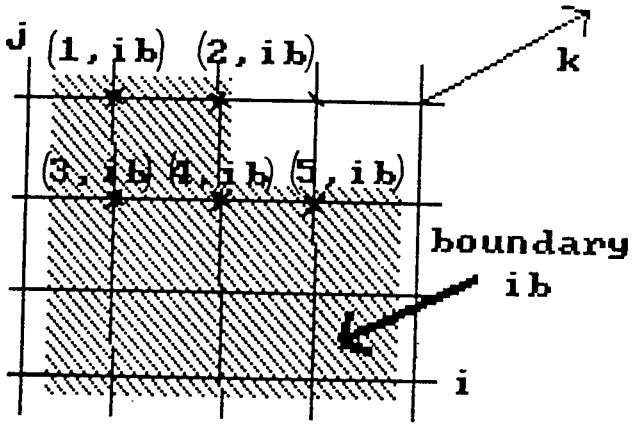

Fig. 1 Geometrical definition (indexing) of boundaries.

The same principle could be applied to the case of adiabatic reactions instead of isothermal reactions, as assumed here.

Since MacCormack's scheme is used to solve the governing equations, the source terms $\dot{X}_{i_{react}}$ are evaluated at predictor step and also at corrector step, using the updated values of temperature.

Numerical Methods

The system of governing equations can be put into the form

$$\frac{\partial f}{\partial t} = -\operatorname{div}[F(f)] + S \tag{44}$$

where f is a vector whose n components are the unknowns ρ, $\rho\underline{u}$, ρe_t; X_i the chemical composition, and E^t_{vib} the vibrational energy. Here S is the vector containing n source terms for the components of f. F is a function of f producing a matrix $(n,2)$ in the $2D$ case, corresponding to the flux terms.

To integrate the differential system [Eq. (1)], our scheme is a modification of the classical two-step explicit method of MacCormack.[15] These classical two steps are replaced in our computer code by three steps. The first two steps are strictly symmetrical, and thus allow use of the same subroutine to evaluate the new value at predictor and corrector steps. The last step is an averaging step. The splitting of a corrector time step into two substeps is just a gimmick. The final result is exactly the same as with the original MacCormack's solver, and it retains the same precision and properties.

$$f_p^{n+1} = f^n - [\overline{\mathrm{DIV}}_F(F(f^n)] - S^n)\,dt \tag{45}$$

$$f_c^{n+1} = f_p^{n+1} - [\overline{\mathrm{DIV}}_B(F(f_p^{n+1})] - S_p^{n+1})\,dt \tag{46}$$

$$f^{n+1} = \tfrac{1}{2}(f^n + f_c^{n+1}) \tag{47}$$

DIV_F and DIV_B represent forward and backward discretization of the divergence operator, subscript p refers to predicted values, subscript c refers to corrected values, superscript n indicates the time step at which the values are evaluated.

To increase the versatility of the code, a zonal approach similar to the one used by Veuillot and Meauze[23] has been introduced. The computational domain D can be decomposed into subdomains $D_1, D_2, \ldots, D_m$. In each of the subdomains, different densities of grid points can be used. To allow an easy definition of complex shapes and boundaries, an indirect addressing technique is used (Fig. 1). Two integer arrays store the indices $i_{bo}(n,i_b)$, $j_{bo}(n,i_b)$ of the nth point of the boundary i_b. The artificial boundaries (connection between two domains) are defined in the same manner.

This technique can be extended to three-dimensional codes (Fig. 1). It allows the use of the code for internal as well as external flows, with very simple changes in the set of input data.

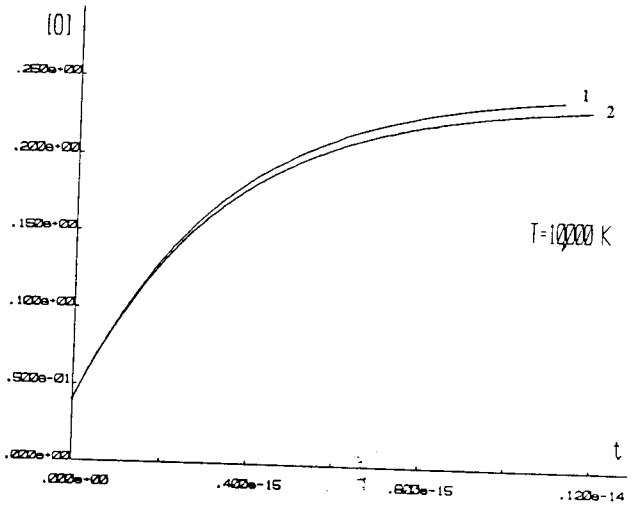

Fig. 2 Validation of the ODE solver for the time evolution of atomic oxygen: 1) analytic; 2) Newton's iteration.

At the current time, eight types of boundaries have been introduced in the code. They are: inlet, isothermal wall, adiabatic wall, exit, secondary inlet (to simulate injection of chemical species in the field), connection between domains, far field, and symmetry.

Results

Before running the code, it is necessary to assess the validity of the chemical kinetics solver. Therefore, the subroutine used to predict the evolution of species concentration, with Newton's iteration technique, has been tested separately. These results have been compared with the theoretical curves obtained by plotting time vs the evolution of concentration that is given explicitly by Eq. (31). This test has been done for the dissociation of O_2 (Fig. 2) and the dissociation of N_2 (Fig. 3). In both cases the solver proved to be accurate and very fast.

Then, the complete hypersonic flow analysis code was applied to three different test cases. For all three cases, the geometry is a rectangular box (Fig. 4), closed and filled with a mixture of molecular nitrogen, N_2, and with atomic nitrogen, N. The walls were treated as isothermal and noncatalytic.

For the first test case, the nonpartitioned box is filled with a mixture of N and N_2 at a given uniform temperature T and pressure P. Nevertheless, the initial concentrations of N_2 and N do not correspond to equilibrium composition for the initial pressure and temperature. A very small time step is therefore chosen, adapted to the chemical reactions ($\Delta t = 1\mathrm{E}-18$ s). The temperature and pressure of the mixture increase and, in turn, the equilibrium composition is modified. A steady equilibrium is finally reached, as shown by the plot of pressure vs time at a point near the vertical walls (Fig. 5). The recombination of N yields a final pressure and temperature higher than their initial values.

In the second test case, the box is initially partitioned by a membrane. The zonal approach was used to discretize each of the two halves of the box. Uniform coarse computational grid was used in both domains, with overlapping cells at the location of the membrane (Fig. 4). The pressures and temperatures on the two sides of the box were the same, but the compositions were different. For this test case, we froze the chemical reactions; that is, we imposed a species production term always equal to zero. In this situation, the possible physical phenomena are limited to diffusion and convection only. These processes are considerably slower than the chemical reactions, as the flow is nearly motionless; therefore, a

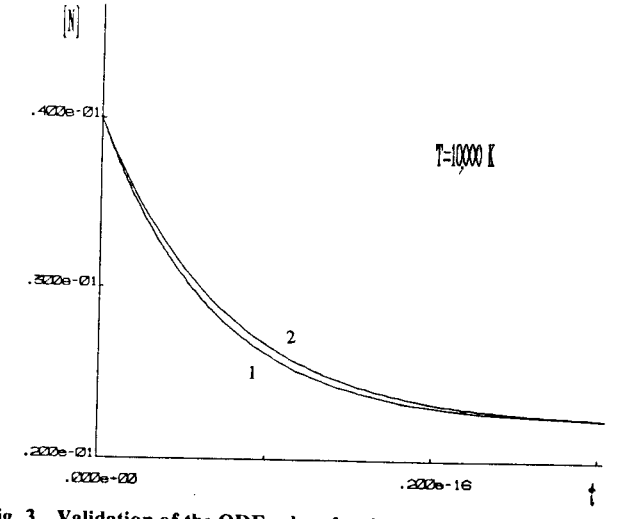

Fig. 3 Validation of the ODE solver for the time evolution of atomic nitrogen: 1) analytic; 2) Newton's iteration.

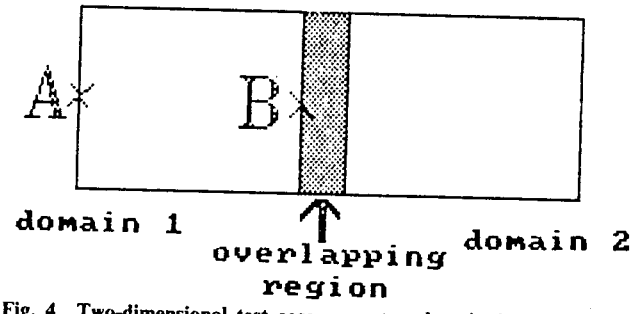

Fig. 4 Two-dimensional test case geometry: domain 1 and domain 2 are unit squares.

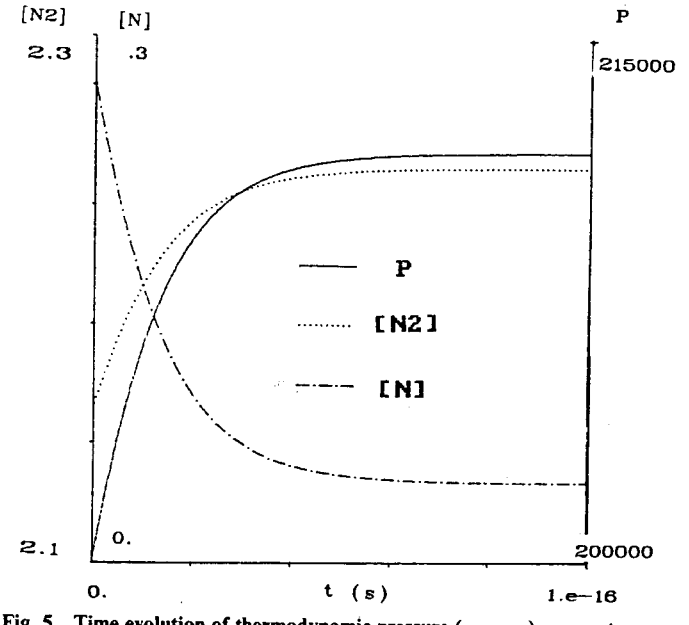

Fig. 5 Time evolution of thermodynamic pressure (———), concentration of molecular nitrogen (.....), and concentration of atomic nitrogen (- - - - -) having a uniform initial composition.

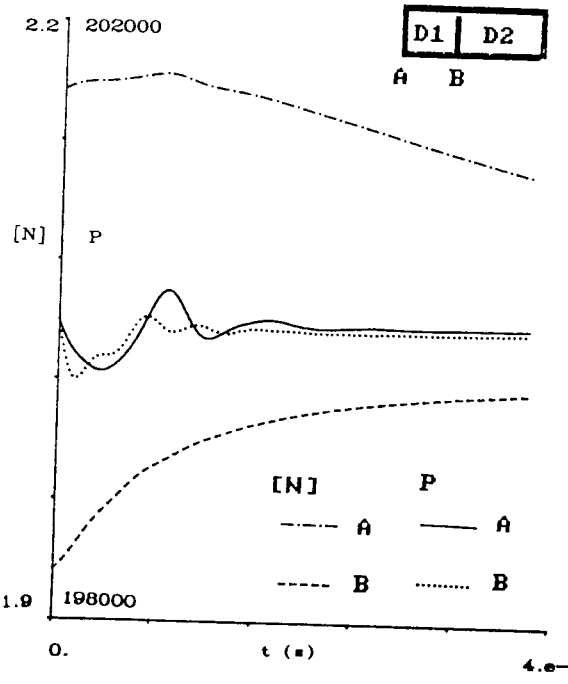

Fig. 6 Time evolution of thermodynamic pressure and concentration of atomic nitrogen at the left wall (A) and at the midsection (B) for nonuniform initial composition (frozen chemistry).

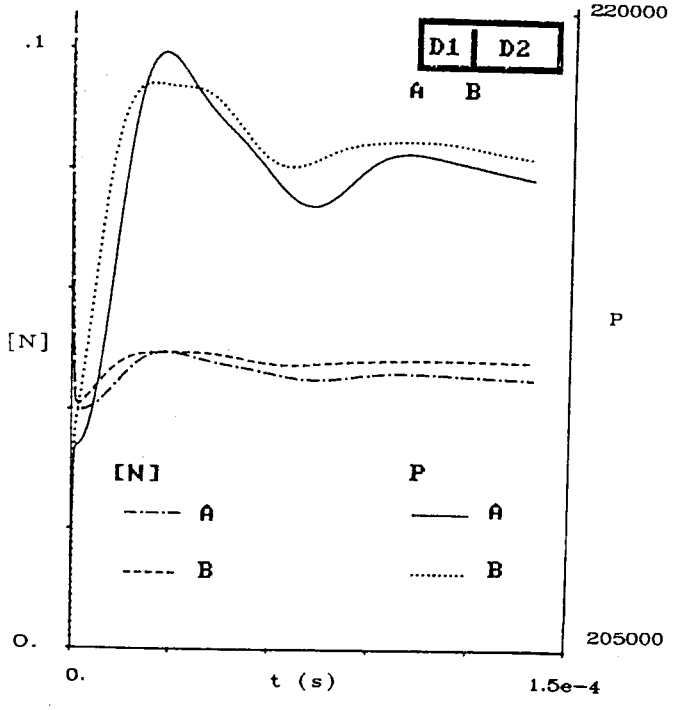

Fig. 7 Time evolution of thermodynamic pressure and concentration of atomic nitrogen at the left wall (A) and at the midsection (B) for nonuniform initial composition (equilibrium chemistry).

much larger total time is needed to reach the equilibrium. As expected, the concentrations of N_2 and N tend to become uniform in the box (Fig. 6), and the pressure returns to its initial value.

The third test case differs from the second case only by taking into account the equilibrium chemistry. The diffusion of mass, momentum, and energy is a relatively slow process. The convective terms also appear. Thus, the main effect is caused by the chemical reactions. The initial condition corresponds to a mixture with a concentration of N that is higher than the equilibrium value for the local pressure and temperature. Thus, the atoms of N will tend to recombine, as in the first test case. At $t = 0$, pressure and temperature are the same on both sides of the membrane. But the density and molar masses are different, since they correspond to different equilibrium compositions. In turn, the heat released by the chem-

ical reactions on the two sides of the membrane will be different for $t > 0$. Therefore, strong gradients of pressure and temperature appear. As a result, an acoustic wave develops and propagates into the box,[6] as shown in Fig. 7. The frequency of this wave corresponds clearly to the first longitudinal mode of excitation of the box. A strong damping of the wave also can be observed in Fig. 7. The last part of the curve corresponds to convection and diffusion processes, tending to produce a uniform temperature and composition. This computation is performed with quite a large time step ($\Delta t = 2E - 7$ s). One thousand iterations, for 110 grid points, took 8 min on a VAX 8550. It should be pointed out that even though this test case corresponds to equilibrium chemistry, we let the complete hypersonic flow analysis computer program compute the source terms as the limit of nonequilibrium chemistry source terms.

Summary

A block-structured computer code was developed that is capable of predicting unsteady convective processes arising from chemical reactions involving nitrogen and the unsteady convective processes resulting from a pure diffusion of nitrogen atoms and nitrogen molecules. In general, the computer code is capable of predicting hypersonic unsteady laminar flows with nonequilibrium chemistry of air. It allows for computational grid movements and multiple domains. An efficient and accurate computation of chemistry is demonstrated that is based on a special variable transformation.

Acknowledgments

This research has been supported by NASA Ames Grant NCA 2-120, and by Direction des Recherches, Etudes et Techniques, under Contract 85.34.1385, while Mr. Lionel Marraffa was a Visiting Research Scientist at the Pennsylvania State University. Special thanks are due to Ms. Amy Myers for her superb typing, and to Dr. Chul Park and other colleagues at NASA Ames Research Center for the valuable discussions.

References

[1]Waldberg, G. D., "A Survey of Aeroassisted Orbit Transfer," *Journal of Spacecraft and Rockets*, Vol. 22, Jan.–Feb. 1985, pp. 3–18.

[2]Howe, J. T., "Introductory Aerothermodynamics of Advanced Space Transportation Systems," *Journal of Spacecraft and Rockets*, Vol. 22, Jan.–Feb. 1985, pp. 19–26.

[3]Anderson, J. D., Jr., "A Survey of Modern Research in Hypersonic Aerodynamics," AIAA Paper 84-1578, June 1984.

[4]Park, C. "Radiation Enhancement by Nonequilibrium in Earth's Atmosphere," *Journal of Spacecraft and Rockets*, Vol. 22, Jan.–Feb. 1985, pp. 27–36.

[5]Balakrishnan, A., "Computation of a Viscous Real Gas Flowfield for the Space Shuttle Orbiter," AIAA Paper 84-1748, June 1984.

[6]Green, M. J., Davy, W. C., and Lombard, C. K., "CAGI2-A CSCM Based Procedure for Flow of an Equilibrium Chemically Reacting Gas," AIAA Paper 85-0927, June 1985.

[7]Montagne, J. L., "Use of an Upwinded Scheme for Simulating Nonviscous Flows of Real Gas at Equilibrium," *La Recherche Aerospatiale*, No. 6, Nov.–Dec., 1986.

[8]McWherter, M., Noack, R. W., and Oberkampf, W. L., "Evaluation of Boundary-Layer and Parabolized Navier–Stokes Solutions for Re-Entry Vehicles," *Journal of Spacecraft and Rockets*, Vol. 23, Jan.–Feb. 1985, pp. 70–78.

[9]Gnoffo, P. A., McCanlers, R. S., and Yee, H. C., "Enhancements to Program LAURA for Computation of Three-Dimensional Hypersonic Flow," AIAA Paper 87-0280, Jan. 1987.

[10]Mani, M., Tiwari, S. N., and Drummond, J. P., "Numerical Solution of Chemically Reacting and Radiating Flows," AIAA Paper 87-0324, Jan. 1987.

[11]Chitsomboom, T., Kumar, A., and Tiwari, S. N., "Numerical Study of Finite-Rate Supersonic Combustion Using Parabolized Equations," AIAA Paper 87-0088, Jan. 1987.

[12]Prabhu, D. K., Tannehill, J. C., and Marvin, J. G., "A New PNS Code for Chemical Nonequilibrium Flows," AIAA Paper 87-0284, Jan. 1987.

[13]Park, C., "Assessment of Two-Temperature Kinetic Model for Dissociating and Weakly-Ionizing Nitrogen," AIAA Paper 86-1347, June 1986.

[14]Carcaillet, R., Dulikravich, G. S., and Kennon, S. R., "Generation of Solution-Adaptive Computational Grids Using Optimization," *Computer Methods in Applied Mechanics and Engineering*, Vol. 57, Sept. 1986, pp. 279–295.

[15]MacCormack, R. W., "The Effect of Viscosity in Hypervelocity Impact Cratering," AIAA Paper 69-354, 1969.

[16]Brackbill, J. U., "Numerical Magnetohydrodynamics for High Beta Plasmas," *Methods in Computational Physics*, Vol. 16, 1–41, Academic, New York, 1976.

[17]Miner, E. W. and Lewis, C. H., "Hypersonic Ionizing Air Viscous Shock Layer Flows Over Nonanalytic Blunt Bodies," NASA CR-2550, 1975.

[18]Wilke, C. R., "A Viscosity Equation for Gas Mixtures," *Journal of Chemical Physics*, Vol. 15, April 1950, pp. 517–519.

[19]Vincenti, W. G. and Kruger, C. H., Jr., *Introduction to Physical Gas Dynamics*, Robert E. Krieger Pub., Huntington, NY, 1975.

[20]Rakich, J. V., Bailey, H. E., and Park, C., "Computation of Nonequilibrium Supersonic Three-Dimensional Inviscid Flow Over Blunt-Nosed Bodies," *AIAA Journal*, Vol. 21, June 1983, pp. 834–841.

[21]Gear, C. W., *Numerical Initial Value Problems in Ordinary Differential Equations*, Prentice-Hall, Englewood Cliffs, NJ, 1971.

[22]Radhakrishnan, K., "Integrating Chemical Kinetic Rate Equations by Selective Use of Stiff and Nonstiff Methods," NASA TM-86923, 1985.

[23]Veuillot, J. P. and Meauze, G., "A 3D Euler Method for Internal Transonic Flows Computation with a Multidomain Approach," AGARD LS-140, 1985, pp. 5.1–5.21.